

DOPPLER IMAGING OF SPOTTED STARS: APPLICATION TO THE RS CANUM VENATICORUM STAR HR 1099*†

STEVEN S. VOGT AND G. DONALD PENROD

Lick Observatory, Board of Studies in Astronomy and Astrophysics, University of California
Santa Cruz, California 95064

We discuss a technique for imaging the surfaces of certain rapidly rotating spotted stars. The method exploits the correspondence between wavelength position across a rotationally broadened spectral line and spatial position across the stellar disk. Preliminary Doppler Images of the RS CVn star HR 1099 show spots which exhibit a striking similarity in shape and location to X-ray images of solar coronal holes. We suggest that the large star spots on RS CVn's and other active late-type stars emerge at low latitude as scaled-up stellar analogs of solar complexes, but as they migrate poleward, they more closely resemble photospheric analogs of solar coronal holes. The evolution of starspots appears remarkably similar to that of large-scale magnetic fields of the sun.

Key words: RS CVn binaries—BY Dra stars—stellar surface activity—stellar rotation—sun: corona—sun: magnetic fields—sun: activity cycles

I. Introduction

There are now at least three groups of stars which are believed to have large cool spots on their surfaces. These spots are inferred mainly from periodic variations in a star's integrated light as these dark regions are carried into and out of view by the rotation of the star. The most well-known examples of spotted stars are the RS Canum Venaticorum and the BY Draconis stars. Extensive literature on the spotted nature of both of these groups now exists, and no attempt will be made here to review their basic properties. A recent attempt to review the subject of starspots was presented by Vogt (1982), and a good discussion of spots on the RS CVn's was given by Hall (1976). The third and most recently discovered group of spotted stars includes the periodically variable pre-main-sequence K-stars (Rydgren and Vrba 1983), and Pleiades member K-stars (Van Leeuwen and Alphenaar 1982).

Through modeling of the photometric variations, it has become clear that starspots are often quite large, covering up to 20% of the stellar surface. In most well-determined cases the spot temperatures are near 3600 K. There is evidence that some spots prefer intermediate to high latitudes, in one case even straddling the pole of the star. While modeling of the photometric variations has yielded good estimates of spot sizes and temperatures, the solutions are fraught with uniqueness problems. The spot models are always highly idealized (invoking one or two circular spots, etc.) and the modeling attempts usually degenerate to demonstrating that a particular as-

sumed spot configuration is consistent with the observed photometric variations. We seem to have neared the limit of information regarding detailed spot shapes, locations, and movements which can be extracted from the broad-band photometry.

Several years ago, Fekel (1980) noticed distortions in the absorption lines of the spotted RS CVn star HR 1099, which seemed to be correlated with orbital phase. Upon learning of this discovery, it occurred to us that these distortions were essentially one-dimensional maps of the surface brightness of the rotating star. If enough phases could be suitably combined, and the inclination of the star was known, a resolved image of the spotted star should be derivable. We have been working on a technique, called Doppler Imaging (Vogt and Penrod 1982), to generate such images from spectral line profile distortions. This paper presents a more thorough discussion of the Doppler Imaging method and its preliminary application to the spotted star HR 1099. With this technique, we expect to be able to resolve individual spots, and to determine in detail their shapes, locations, and migratory motions. In particular, we would like to know if starspots have umbrae and penumbrae, as do sunspots, and whether or not they occur as bipolar groups. We would also like to know unambiguously where they form on the star, and how they migrate with time.

II. The Doppler Imaging Technique

A. Formation of the Bumps

The Doppler Imaging technique exploits the fact that, in the spectrum of a rotating star, there exists a one-to-one correspondence between wavelength position across any spectral line and spatial position across the stellar disk. This correspondence occurs because lines of constant radial velocity are chords across the disk, parallel

*An invited paper presented at the Symposium on the Renaissance in High-Resolution Spectroscopy—New Techniques, New Frontiers, at the 94th Annual Scientific Meeting of the Astronomical Society of the Pacific, Kona, Hawaii, June 1983.

†Lick Observatory Bulletin No. 969.

to the star's rotation axis. Thus, a mapping occurs in one dimension between position across the disk and wavelength position across any spectral line. Any region of excess brightness or coolness on the surface gives rise to an associated bump or depression in any spectral line profile at the position corresponding to the radial velocity of the region. As the region is carried across the disk by stellar rotation, the associated bump or depression propagates across the line profile.

For stars in which the rotational Doppler broadening is less than or equal to the intrinsic Voigt profile, this mapping effect becomes lost in the uncertainties of the intrinsic line profile. However, for stars with $v \sin i$ equal to or greater than about 30 km s^{-1} the Doppler broadening from rotation can be many times greater than the Voigt profile. The latter can then be easily decoupled from the mapping procedure.

If a spot is much cooler than the surrounding photosphere, it gives rise to an apparent emission bump within a spectral absorption line as Figure 1 illustrates. Here we show a rotating star which is divided into five equal-area zones of approximately constant radial velocity in each zone. The left-hand sequence of profiles illustrates the formation of a spectral line profile in the absence of any spot on the star. For simplicity, the specific intensity profile from each zone is assumed to drop to zero intensity at line center, and the continua are normalized to add to unity in the sum over five zones. Thus the five specific intensity profiles in the left-hand sequence are all identical except for their respective Doppler shifts due to stellar rotation. When these five profiles are added to form the integrated flux profile, the result is a broadened line whose width merely reflects the rapid rotation of the star.

Now consider an absolutely black (zero flux) spot covering exactly 50% of the area of region III as shown. The right-hand series of profiles shows the appropriate specific intensity profiles for this spotted geometry. The result of summing these profiles is a broadened absorption line as before, but with an apparent emission bump in the center. Obviously, this bump does not represent true emission, but rather a *lack* of line absorption at the radial velocity corresponding to the spotted zone III. As such, this "emission" bump would never rise above the local continuum. Notice that the intrinsic line profile from zone III has not changed, but the continuum flux has changed since one-half the area is covered by a black spot. So there exists, at this velocity, a net lack of photons absorbed by the line, and thus an *apparent* emission bump. The effect is purely a geometric one, and bumps would appear almost identically in all of the star's absorption lines.

In actuality, the situation is much more complex. Here we considered only a zero-flux spot. If the spot's temper-

ature is nonzero, its intrinsic spectrum must also be considered. The important quantity then becomes the product $F \times W$, where F is the continuum flux at a particular region on the star, and W is the local equivalent width of the spectral line. Defining F and W as the flux and equivalent width for the normal stellar photosphere, and f and w as the same for the spot's photosphere, if $(f \times w) < (F \times W)$ an emission bump appears. If $(f \times w) > (F \times W)$ an absorption dip appears on the line profile. If $(f \times w) = (F \times W)$ no distortion occurs on the line profile. The analysis is further complicated by the fact that F , W , f , and w are all functions of limb angle, and this limb angle dependence is different for a cool starspot than for its hotter surrounding photosphere. So, cool spots can appear more visible (i.e., stronger bump) when near the limb than near disk center. While these factors do complicate the analysis, we intend to exploit them to provide more detailed information on spot temperatures and locations.

B. Requirements for Doppler Imaging

To be Doppler Imaged, a star must be rotating rapidly enough that its linewidths are dominated by rotational broadening. For the RS CVn's and BY Dra's, a $v \sin i$ of at least $25\text{--}30 \text{ km s}^{-1}$ is required. Faster rotation rates are desirable since the spatial resolution obviously increases with rotational velocity. However, since line equivalent widths are, to first order, conserved under rotational broadening, more rapid rotation results in smaller line depths, and thus a higher signal-to-noise ratio is required to detect a bump which is some constant fraction of that line depth. Above about 100 km s^{-1} , the broadened lines become so shallow that distortions on their profiles become difficult to distinguish from the myriad of unidentified telluric features almost always present. Obtaining high enough signal-to-noise ratios to detect such weak bumps also becomes a real limitation. For this reason, intermediate rotational velocities of 40 to 80 km s^{-1} are optimum for Doppler Imaging.

As will be shown, even the largest bumps found in the absorption lines of spotted stars are only about 3% to 4% of the continuum. Typical bumps are only about 1% of the continuum. Thus, a signal-to-noise ratio of at least 100 is necessary. To take full advantage of the spectral information present in such profiles, an instrumental resolution of at least 40,000 is needed. We typically work near 6400 \AA with a wavelength resolution of 0.1 \AA , and a signal-to-noise ratio of at least 200.

Any single observation yields only one dimension of spatial information across the disk. Acquiring the second spatial dimension requires a suitable stellar inclination, and a coherent series of observations which can be phased together as one data set. Obviously, if the inclination is 0° (pole-on) no Doppler broadening is seen

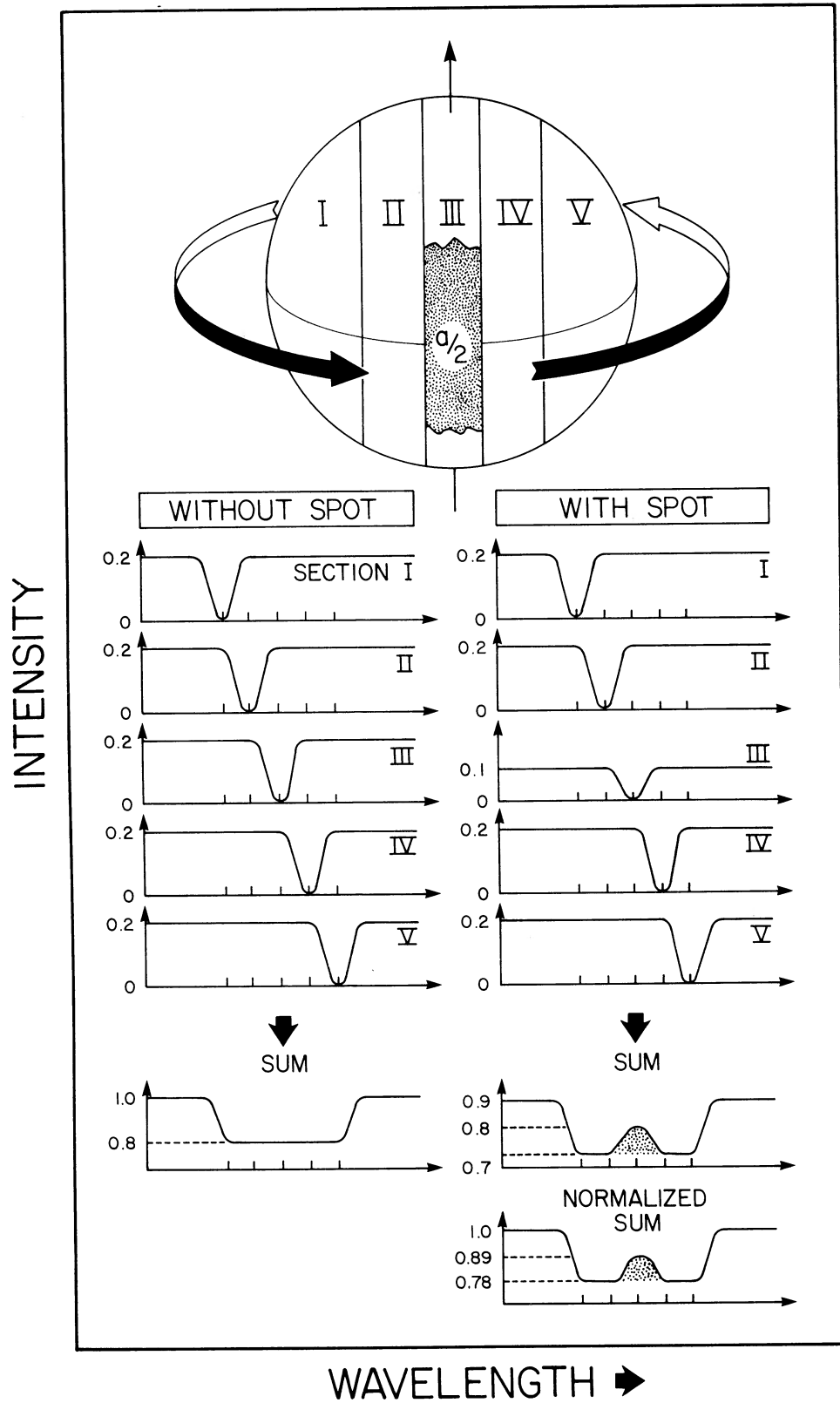


FIG. 1—Illustration of the formation of apparent emission bumps in the absorption lines of a rapidly rotating spotted star.

and Doppler Imaging is impossible. If the inclination is 90° , an ambiguity arises as to which hemisphere (north

or south) a spot belongs. Here, the mapping becomes highly nonunique in the direction parallel to the rotation

axis. However, for intermediate inclinations (45° is optimum), an adequate amount of rotational broadening is present, while at the same time the lower hemisphere is mostly hidden from view so as not to complicate the modeling. In this case, some 2-d information on the visible hemisphere is obtainable, as will be shown.

Obviously, the better the phase coverage, the better will be the final Doppler Image. In practice, it is difficult to obtain enough of the right type of observing time on a single large telescope to obtain more than a dozen or so distinct phases within any two- to three-month interval over which the spots can be assumed to be constant. Over longer time intervals than this, spots on the RS CVn's and BY Dra's evolve discernibly, making it difficult to combine the line profiles in the analysis. Fortunately, 6–10 observations uniformly spread over rotational phase space are adequate to produce a reasonably valid map of the spot distribution. The task of obtaining adequate phase coverage would be greatly facilitated by collaboration among several observatories.

A very critical requirement is the need to find clean unblended spectral lines. Since many spotted stars occur as double-lined spectroscopic binaries, this is not easily done. For late-type stars, the blue region of the spectrum is hopeless due to severe line blending. In the red, the line blending is less problematical, but at the expense of a relative dearth of strong lines and contamination problems from terrestrial lines. The best region we have found for the G and K stars is near 6400 \AA . In particular, Fe I at 6430.9 \AA and Ca I at 6439.1 \AA are quite usable. Ideally, the lines should not be too temperature sensitive, as this greatly complicates the imaging process. In this regard, the Ca I line at 6439.1 \AA is less than optimum since calcium is almost completely ionized in the normal stellar photosphere, but almost completely neutral in the spot. Thus the line strength increases dramatically from photosphere to spot, and partially offsets the drop in continuum flux from photosphere to spot. The net result of this is a considerable weakening of the bump in this line.

It is quite useful to have good broad-band light curves at the epoch of the spectral observations for additional constraints on the imaging. The line-profile distortions are not as sensitive as the photometry to total spot area, but are much more sensitive to the detailed shapes and latitude extents of spots. Indeed, a spot group with a very small latitude extent, but large longitude extent could produce a large-amplitude light curve with only subtle variations in the line profiles. It is thus important to combine *both* the broad-band photometry *and* the line profiles in the imaging process.

At this point, perhaps a plea to photometrists is in order. Good photometric coverage of the prime spotted-star candidates has not occurred during the past several

years, though we have been compiling spectral line profiles on several spotted stars over this period. There are, at present, at least six prime spotted stars which should be monitored photometrically every available season for the next several years as more spectral line profiles are accumulated for Doppler Imaging. These candidates are HR 1099, UX Aries, SZ Piscium, AR Lacertae, HD 199178, and HD 26337. These are the brightest Northern Hemisphere spotted stars and will be the subject of intense spectroscopic monitoring from Lick Observatory over the next few years. As time on larger telescopes and improvements in spectroscopic instrumentation permits, fainter stars will also be brought into the observing program. There are also good spotted stars in the Southern Hemisphere which need photometric and spectroscopic coverage.

In Figure 2 we present some examples of bumps in the 6430.9 \AA and 6439.1 \AA lines. These data were obtained with the coude spectrometer of the Shane 3-m telescope at Lick Observatory. The AR Lac observation was taken with a Reticon detector (Vogt 1981a), while the rest were taken with the double-pass echelle and IDS detector (Soderblom 1982). The resolution was 0.15 \AA in the former and 0.1 \AA in the latter. While the IDS spectra are nicely oversampled, they contain only one line per observation. The Reticon spectra cover 100 \AA per observation and contain many lines, allowing intercomparison between several line profiles in a given observation. Then, since any spot produces almost identical bumps in all neutral metal lines, the distinction between real spot signatures and noise wiggles or blends on the line profiles becomes much easier. The Reticon spectra generally can attain a higher signal-to-noise ratio than the IDS spectra, but at the expense of somewhat less resolution and much less sampling.

C. Deriving the Surface Maps

When the stellar inclination is at an intermediate value (30° to 60°), a considerable amount of 2-d information can be obtained from the line profiles, in spite of the fact that each profile represents only a 1-d image of brightness across the disk. For example, a dark spot situated at the pole would produce a bump precisely at line center for all phases. Spots at progressively lower latitudes would produce bumps which exhibit progressively larger excursions from line center, and progressively faster rates of profile crossing. In this way, the latitude of a spot can often be accurately established. Spots at a latitude greater than $90 - i$ (where i is the inclination) are circumpolar and produce bumps which are always in view. We have actually observed spots passing around *behind* the pole on one of our program stars. Information about detailed spot shapes can be derived by exploiting the fact that, at intermediate stellar inclinations,

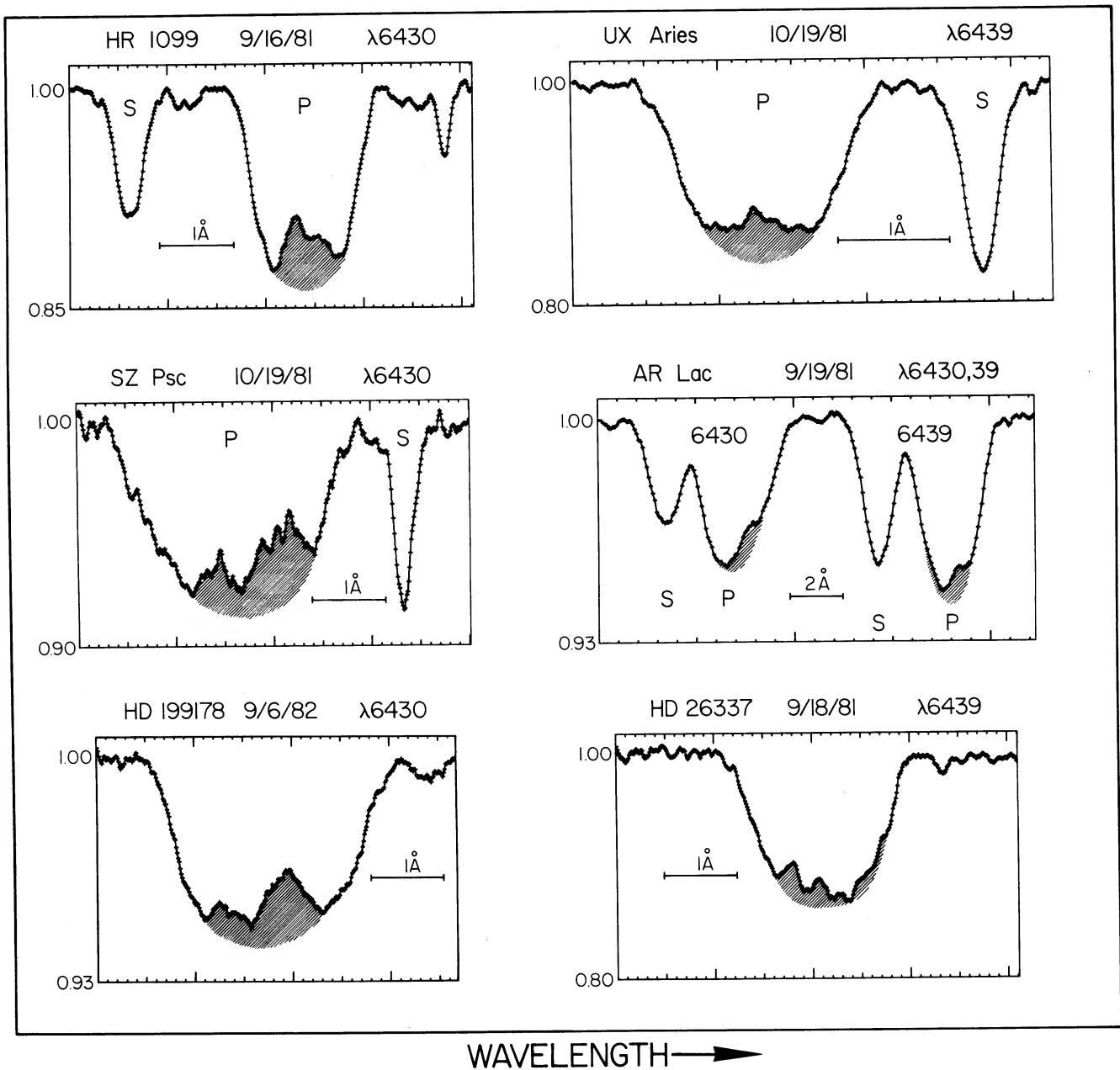


FIG. 2.—A sample of observed line profiles from our spotted program stars.

a given spot rotates as it is carried across the disk. Thus, observations at different phases sample different projections of the spot. In these various ways, a substantial amount of 2-d information can be obtained from a good set of line profiles.

At present, the task of deriving the images of spotted stars is largely an iterative process using a family of interactive line synthesis programs written by one of us (G.D.P.) for the Lick Observatory VAX computer. We generate theoretical spectral line profiles from assumed spot distributions, compare with all observed line profiles and with the light curve, modify the assumed spot

image, and iterate until satisfactory agreement is obtained with all the observational data. First, at least 6–8 high-quality line profiles are obtained, and phased properly together. Major bumps are identified and an attempt is made to distinguish between prominent bumps and to follow their behavior with phase through the line profile set. From this preliminary study of the profiles, an initial guess of the spot image is made. For example, if a prominent bump were present near line center at all phases, one would guess that a large spot very near the pole was present. For computational simplicity and flexibility, the assumed spot distribution is composed as the

sum of a large number (up to 50 at present) of smaller circular spots, each with its own assignable longitude, latitude, size, and temperature.

A total of 90 specific intensity line profiles, previously computed for three different temperature LTE atmospheres (umbra, penumbra, and undisturbed photosphere) and for 30 different limb angles across the star, are then accessed to compute the resultant spectral line flux profile. The stellar disk is divided into a rectangular 100×100 grid of zones. At each zone, the appropriate specific intensity profile is selected from the set of 90, according to the local limb angle, and whether the zone occurs in umbra, penumbra, or undisturbed photosphere. Overlapping penumbrae and umbrae are counted as umbra, whereas overlapping penumbrae are still considered penumbra. Once the proper specific intensity profile has been selected for the zone, it is then assigned a Doppler velocity which is the sum of a random component of radial-tangential macroturbulence plus the local radial velocity due to stellar rotation. The Doppler-shifted profile is then co-added into a line-flux summing buffer. This process is repeated for all of the approximately 10,000 zones over the star to produce the intrinsic line-flux profile. This profile is then convolved with our instrumental resolution profile to produce the final result which can be directly compared with an observed line profile. This modeling often fits our high-resolution, very high signal-to-noise ratio spectra to better than 0.5% at all resolution elements across the line. We also keep track of the total flux in the continuum adjacent to the line, to generate a light curve for comparison with observed light curves.

The theoretical line profiles and light curve are then compared in detail with the observations, and deviations of one from the other are used to modify the assumed spot configuration for the next attempt. This iterative process is then repeated (typically 10–15 times) until satisfactory agreement is obtained. The computer modeling is carried out interactively on our VAX computer, and requires only about 2–5 minutes to compute a set of line profiles. Thus, each iteration can be carried out in under 30 minutes, and convergence to a good solution can be achieved in 1–3 days.

We have worried a great deal about solution uniqueness, and have compared Doppler Images derived completely independently from the same profile set by two different people. In such tests, close agreement between the solutions was found, and uniqueness problems seem well under control. Of course, one could probably always find some random distribution of spots across the stellar surface which could fit all the observations. At some level, it becomes necessary to invoke Occam's razor, and make the reasonable assumption that the spots can be characterized as a small number of relatively prominent and distinct areas, rather than a random

mottling of many distinct spots spread quasi-uniformly over the surface. The Doppler Imaging technique would have no hope of characterizing the latter.

III. Doppler Images of HR 1099

Our best candidate for Doppler Imaging is the spotted RS CVn binary HR 1099. This star is one of the brightest of its class ($V = 5.9$, K1 IV + G2 V), has a well-determined and nicely intermediate inclination of $i = 33^\circ$, a $v \sin i$ of 38 km s^{-1} , and has a relatively clean spectrum at 6400 \AA . It was recently the subject of a detailed study by Fekel (1983). In Figure 3, we present a series of profiles of the 6430.9 \AA Fe I and 6439.1 \AA Ca I lines from this star. These data were obtained in September and October of 1981 with the coude echelle and IDS detector of the Lick 3-m Shane telescope. Here, only the top 15% of the continuum is shown, and our wavelength resolution of 0.1 \AA is indicated at the bottom. The phases above each line profile were computed from the orbital ephemeris given by Fekel (1983)

$$\text{HJD} = 2442766.080 + 2.83774E \quad ,$$

where zero phase corresponds to time of conjunction with the primary (K-star) in front. In most cases in Figure 3 only the primary's line profile is shown, however, the secondary's profile can be clearly seen near the right edge at phase 0.588, and off the right edge at phases 0.644 and 0.877; it is blended with the primary profile at phase 0.942. Although we sometimes chose not to include it in Figure 3, the secondary line was always recorded. Because the bumps were always confined to the primary's line profiles, the spots can be unambiguously associated with this K subgiant. No evidence of spots on the G2 V secondary was ever seen.

The line profiles in Figure 3 were modeled using a 100×100 grid of zones across the stellar disk, and a radial-tangential macroturbulence of 4 km s^{-1} . The intrinsic line profiles were computed using the atmospheres of Bell et al. (1976) for the primary, and Kurucz (1979) for the secondary. An inclination of 33° was adopted from the work of Fekel (1983). Our line profile fits indicated a $v \sin i$ of $38 \pm 1 \text{ km s}^{-1}$ for the primary and 13 ± 1 for the secondary.

A preliminary Doppler Image obtained from these line profiles is presented in Figure 4. Here we show the spotted star as it appears at essentially all phases of the observed line profiles. Images at phases 0.300 and 0.349 were omitted. They were essentially redundant with phase 0.298 and provided little additional information for the imaging since Ca I 6439.1 \AA is much harder to interpret than Fe I 6430.9 \AA . Underneath each image is the theoretical line profile computed from the spot shown and these theoretical profiles are to be compared directly with the observed profiles in Figure 3. As can be seen, the agreement between the computed and ob-

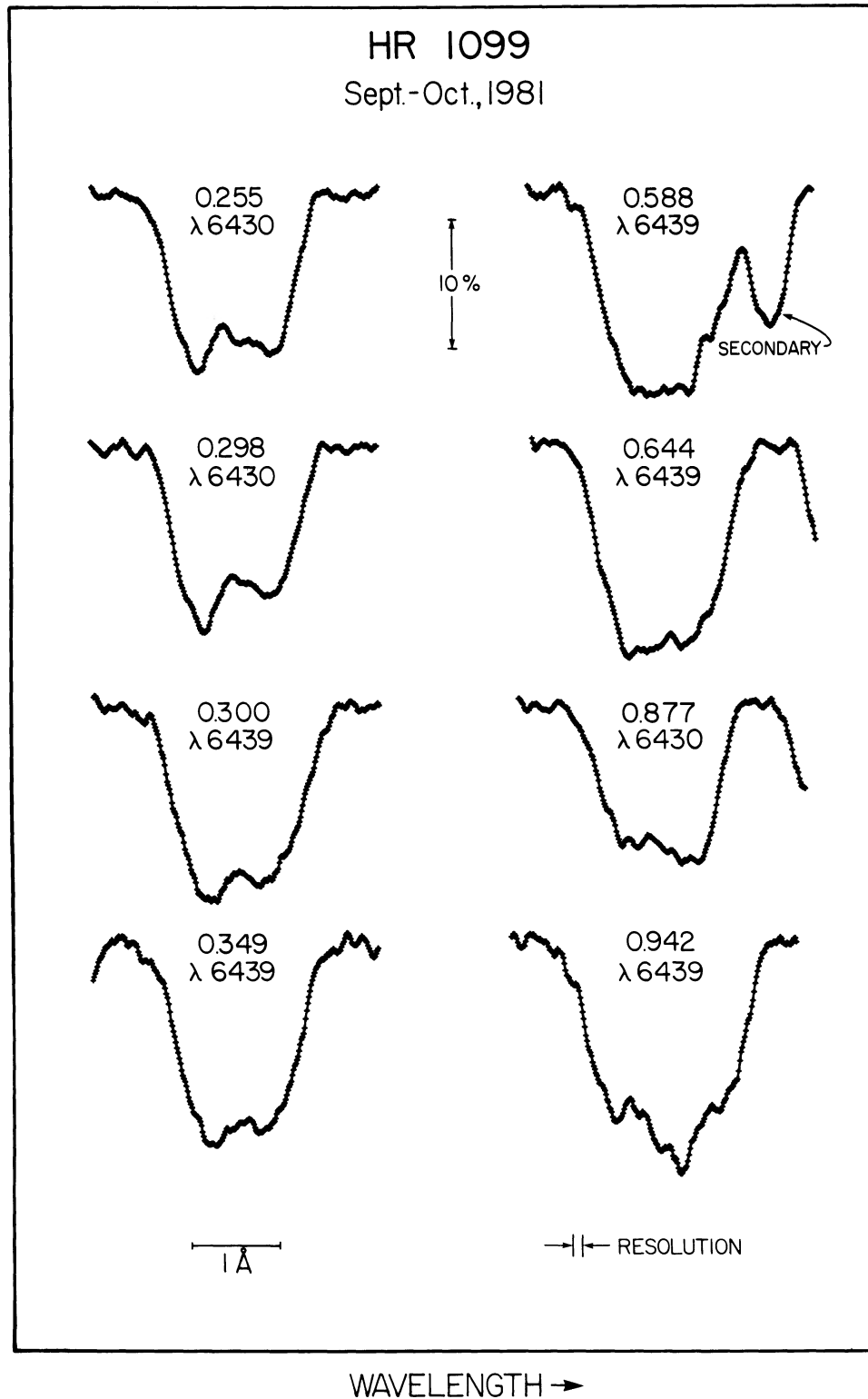


FIG. 3—Line profiles of HR 1099 obtained during Fall 1981.

served profiles is quite good, though further improvement may be possible and the modeling is still in progress. At present, we regard this imaging attempt as preliminary, as we have not yet found simultaneous photometric data to incorporate in the modeling.

The Doppler Images of Figure 4 show two distinct spots separated by roughly 110° in longitude. One spot (hereafter referred to as the polar spot) is a large, approximately circular spot straddling the pole, with an attached narrow lane which descends to about 30° latitude.

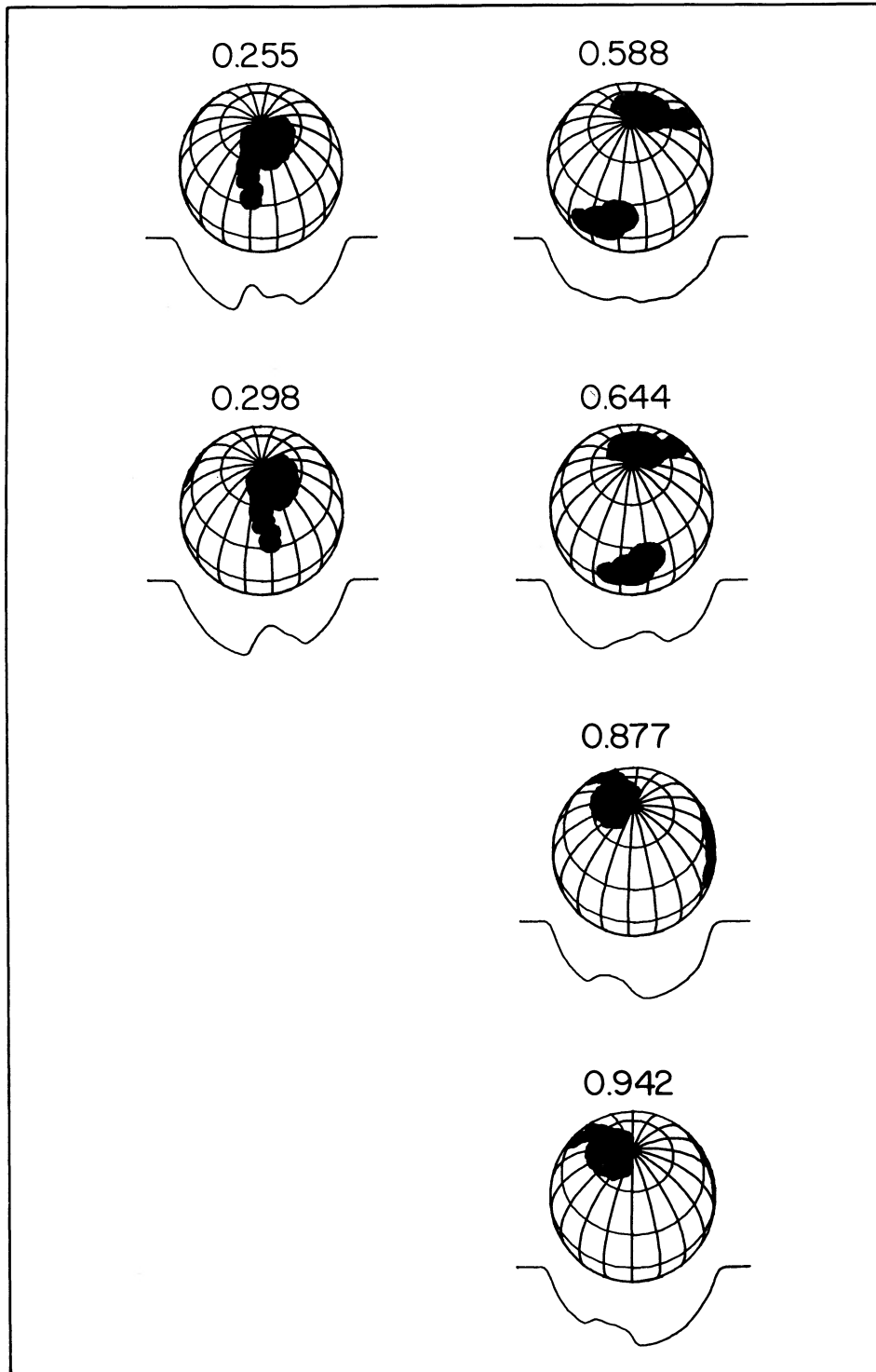


FIG. 4—Doppler Images of HR 1099 derived from the line profiles of Figure 3.

It covered about 8%–10% of the visible hemisphere, and was almost completely circumpolar, remaining nearly fully in view at all rotation phases. Due to the intermediate inclination of the star, it was possible to observe this spot passing around behind the pole from phases 0.5

to 0.9. This spot's shape is quite well-determined because it was almost always in view, and was thus sampled from many angles in the line profile set.

The second spot (hereafter referred to as the equatorial spot) is located at $+12^\circ$ latitude. Its exact size and

shape are less well-determined since it was clearly visible only at phases 0.588 and 0.644. Even at these phases, blending with the polar spot caused some ambiguity. Because of this poor phase coverage of the equatorial spot, it is likely that we have somewhat underestimated its size. This equatorial spot is probably slightly elongated in the longitudinal direction, but the elongation must be regarded as tentative. It may yet be possible to invoke a roughly circular outline for the equatorial spot by some appropriate trade-off with the shape of the polar spot. Further modeling attempts to pin this down are underway. The latitude of the equatorial spot is well-determined from the speed with which this feature crosses the disk, and its longitude is well-determined from the phase of line center crossing.

IV. Discussion

The preliminary Doppler Images of HR 1099 in Figure 4 show two large spots on the star in 1981, one roughly circular spot straddling the pole with a narrow lane descending to intermediate latitudes, and a second, slightly elongated spot located near the equator, approximately 110° away in longitude. Several remarkable, and in some cases, unexpected, conclusions can be drawn from these first images of starspots. First, the existence of a spot which essentially straddles the pole (a polar cap) is now well established from our observations. Less direct evidence for such polar spots was previously presented by Vogt (1981*b*) for the spotted flare star BY Draconis, and has been suspected by others. The present work thus confirms that starspots can exist at much higher latitudes than sunspots, and that they are not disturbed by straddling the pole, a singularity in the rotational velocity field. Second, the narrow lane which descends in latitude from this polar cap has no analog among individual sunspots, or bipolar sunspot groups. It is perhaps better described as a *starstripe* than a *starspot*, and is morphologically quite different from any sunspot or sunspot group. Third, the polar spot bears a striking resemblance as regards shape, size, and location, to X-ray images of solar coronal holes (Timothy, Krieger, and Vaiana 1975).

Solar coronal holes are regions of abnormally low density and temperature in the solar corona. They are most dramatically visible in X-ray images of the sun in the $3 \text{ \AA} - 60 \text{ \AA}$ region, but are also detectable in the visible, near-infrared, and radio regions. They have open magnetic field lines and are known to be the source of high-speed solar wind streams near the ecliptic plane, which in turn cause recurrent geomagnetic disturbances. A good discussion of coronal holes can be found in *Coronal Holes and High Speed Wind Streams* by Zirker (1977).

In particular, the polar spot of HR 1099 looks remarkably similar to solar coronal hole "CH1" discussed by

Timothy et al. (1975). An X-ray photograph of CH1, courtesy of the Solar Physics Group, American Science and Engineering, Inc., Cambridge, Massachusetts, is presented as Figure 5, and shows a $3 \text{ \AA} - 54 \text{ \AA}$ image of CH1 which was obtained on 1973 June 1. Both the HR 1099 polar spot and CH1 show a large polar cap, with an attached narrow lane descending in latitude away from the pole. In fact, large, roughly circular polar coronal holes with narrow 'equatorward' extensions are a very common occurrence among solar coronal holes. The size of the polar hole on the sun is cyclically variable with the eleven-year solar cycle, and is at a maximum during sunspot minimum.

Pursuing the analogy further, starspots and solar coronal holes both exhibit almost rigid-body rotation, and their structures are only weakly affected by differential rotation. They also show a slow poleward drift with time. Vogt (1981*b*) and Oskanyan et al. (1977) have presented evidence that a large dark spot of 1965 on BY Dra initially formed at an intermediate ($40^\circ - 60^\circ$) latitude, and subsequently drifted poleward over the next several years before dissolving and leaving a bright remnant near the pole. This poleward migration and decay of a starspot into a bright active region is quite similar to the gradual disappearance of the polar coronal hole of the sun, and the associated poleward migration of the "coronal polar activity zone" as described by Waldmeier (1981).

We believe that starspots are stellar analogs of solar *complexes* of activity (Bumba and Howard 1965), as Hall (1976) has argued. Howard and Švestka (1977) describe in detail the evolution of a large solar complex which developed during the Skylab mission in 1973. Over a period of about six months, 20 separate *active regions* emerged in a large unipolar magnetic region (UMR) straddling the equator. Intense flare activity and brightening of X-ray loops often accompanied the emergence of new magnetic flux, and for about two months the complex was a strong source of energetic particles. The interconnection of X-ray loops among different active regions, and the occasional simultaneous brightening of several loops associated with different active regions, suggests that the complex as a whole was a single magnetic structure rooted and connected beneath the photosphere. The final decay of the complex was marked by the collapse of the coronal loop system and the formation of a large coronal hole over the remnant field.

Levine (1982) argues that most open magnetic field structures on the sun are intimately associated with active regions. Coronal holes form in the centers of UMRs when the longitude extent of a particular magnetic cell becomes wider than about 30° (Levine 1977). The polarity imbalance necessary to sustain the open fields is maintained by the emergence within the cell of large ac-

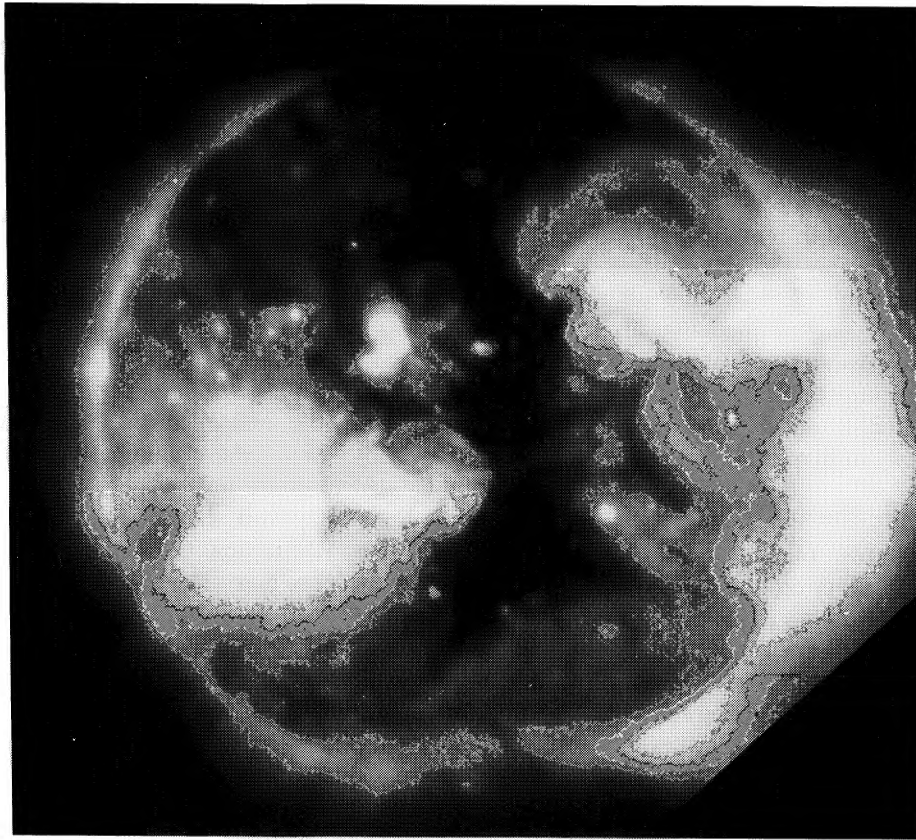


FIG. 5—X-ray photography of coronal hole “CH1”. This is a reproduction of Figure 3a of Timothy et al. (1975). CH1 was the first coronal hole observed during the Skylab mission, and shows the characteristic features of a large polar cap, with an attached narrow descending lane.

tive regions with the proper location and orientation; the fields of the emerged active regions gradually dissolve into the background field of the UMRs. Harvey, Sheeley, and Harvey (1982) suggest that as much as 80% of the sun’s net magnetic flux near sunspot maximum is contained in equatorial coronal holes, with a typical average net field of 10–20 G. The fields of the UMRs are generally carried poleward at a rate of 5–20 m s^{-1} (Howard and Labonte 1981), gradually merging with the field of the polar cap.

We believe that in the last six years we have seen a remarkable analog of the evolution of solar complexes on HR 1099, but on a vastly grander scale. In eight months in 1978 the amplitude of the light variation grew from only 0.08 mag in V (Chambliss et al. 1978) to 0.2 mag (Sarma and Ausekar 1980). Strong radio outbursts (Feldman et al. 1978; Feldman, MacLeod, and Andrew 1979) were detected during this time, and Guinan et al. (1979) reported the observation of a long-lasting flare-like event in optical photometry. This sudden impulse of activity, and the development of a large photometric amplitude, argue very strongly that a new complex of activity emerged during this time near the equator of HR 1099, composed not of 20 active regions but of

20,000, if the scale of individual active regions on HR 1099 is similar to those of the sun. Dorren and Guinan (1982) have attempted to fit these large-amplitude light curves of HR 1099 with a model invoking two circular spots near the stellar equator. The latitude and longitude extent they derive for their “spots” is similar to that of large solar complexes; the “filling factor” of spot umbrae in the complex on HR 1099, however, must be nearly 100%, or several hundred times that of a solar complex.

The polar spot which we observe is clearly the remnant of this large equatorial complex that emerged three years earlier. The dark lane makes its meridian passage at roughly phase 0.25; this agrees very well with the extrapolation of the migration curve presented by Bartolini et al. (1983). During the period from 1979 to 1981 the amplitude of the light curve steadily decreased as the spot moved poleward (Dorren and Guinan 1982; Bartolini et al. 1983). The poleward drift velocity we derive is about 30 m s^{-1} , in rough agreement with that found for solar UMRs.

The striking resemblance between our polar spot and a solar coronal hole suggests to us that they are simply different manifestations of the same phenomenon. The

total amount of magnetic flux that emerges in the evolution of a large solar complex is of order 10^{23} Mx. The diffusion of this flux over a solar magnetic cell produces an average surface field of only 10–20 G, which can have only negligible effect in the photosphere. It is only in the corona, where the densities are much lower, that the weak field can significantly affect the plasma motions. Hence, on the sun open field regions are inconspicuous photospheric structures, but they dominate the structure of the corona.

The magnetic flux needed to create the enormous complex which appeared on HR 1099 in 1978 is of order 10^{26} Mx. This flux is large enough to create *kilogauss* fields over an entire magnetic cell, if the cells are similar in extent to those on the sun. These fields are strong enough to dominate the convective motions which transport heat to the surface over the whole extent of the cell. Hence, the remnant fields of complexes on HR 1099 and other spotted stars may form nearly black “photospheric holes”, which are carried poleward to form a nearly permanent photospheric polar crown similar to that of the sun’s corona. Because of the sizes of these cells, turbulent dissipation of the fields can only gradually reduce the polar spot. The time scale for dissipation is $\tau \simeq L^2/\eta$ where L is the characteristic size scale of the spot and η is the turbulent diffusivity; this time scale is of order 10–100 years for both the RS CVn and BY Dra stars. Indeed, observations of the nearly pole-on spotted BY Draconis star Gliese 171.2A (Hartmann et al. 1981) suggest that the polar spot on this star fluctuates with a time scale of about 60 years.

If *high-latitude* starspots are more nearly analogous to coronal holes than to active regions, as we suggest, then the correlation between the photometric behavior of a spotted star and the other signs of stellar activity (X-ray emission, flares, chromospheric emission, H α emission, etc.) may be much weaker than normally assumed. We suspect that these signs of surface activity mark only the regions of *emerging* flux, and hence are more confined to the equatorial regions. The photometric behavior of the star may, however, be dominated by the quiescent polar spot. Walter, Gibson, and Basri (1983) have recently resolved coronal structure in the eclipsing RS CVn system AR Lac. They find that the X-ray emission from both stars is highly confined to the equator, and probably requires the existence of about 10^6 small coronal loops on each star. They attribute the bulk of the photometric variations, however, to the G-star, on the assumption that the brighter coronal hemisphere and the brightest plage region should be coincident with the darker optical hemisphere. Contrary to this expectation, our observations of AR Lac show that the spectral line asymmetries and hence dark spots are most evident on the K-star (e.g., Fig. 2). If these asymmetries are caused by a

large polar spot, as with HR 1099, then the observations of Walter et al. suggest that a dark starspot can exist in regions almost totally devoid of X-ray emission!

In summary, we suggest the following scenario for the formation and evolution of starspots. Starspots first appear at low latitudes as scaled-up analogs of solar *complexes*, but with a much larger filling factor of dark umbrae due to the vastly larger amount of magnetic flux emerging. This emergence of new magnetic flux causes flaring, enhanced radio and X-ray emission, chromospheric emission, and all of the other phenomena we normally associate with solar *active regions*. This activity declines with time as the mixed fields become more organized through reconnection, drift, and diffusion. The end result of this organization is the formation of open field magnetic structures similar to solar *coronal holes* but with vastly greater magnetic flux. The field strength in these regions is probably similar to that found in sunspot umbrae and is sufficient to dominate gas motions down in the photosphere as well as in the corona. Thus, the region resembles a solar *coronal hole* but is readily visible at optical as well as X-ray wavelengths. With time, these open field regions migrate to the poles where they accumulate to form quite large, long-lived polar spots. Thus, starspots on the RS CVn’s and other active late-type stars can be simply understood as a precise stellar analog of the emergence and evolution of large-scale fields on the sun, though on a much grander scale.

V. Future Directions

In the future, we intend to extend the Doppler Imaging technique to fainter spotted stars and to other studies of stellar surfaces. A prism-cross-dispersed echelle spectrograph and CCD detector now under development at Lick should allow us to acquire suitable line profiles for Doppler Imaging to at least $V = 10$. With this instrument, we will obtain many hundreds of angstroms in a single observation, and hope to be able to use many lines simultaneously to improve our signal-to-noise ratio. These developments will allow imaging of spots on many more RS CVn’s, on pre-main-sequence stars, and on W Ursae Majoris stars. One should be able to study eclipsing systems as well, using the occulting star as an additional mapping probe. Careful studies of the line profiles of rapidly rotating eclipsed stars should provide detailed information on the limb angle behavior of the specific intensity profile and thus direct information about the structure of the atmosphere.

We are using a variation of the Doppler Imaging technique to study the surface velocity fields of rapidly rotating early-type stars. On at least one star, we have detected very high-order nonradial oscillation. This work (Penrod and Vogt 1983) will be presented elsewhere in the meeting. A polarimeter is also being commissioned

for use with the existing echelle/IDS system to allow polarized Doppler Imaging studies of spotted stars in an attempt to detect magnetic fields in and around the spots directly.

Finally, we are exploring ways to automate the iteration process considerably by using techniques which are similar to those developed for CAT scanning in the medical industry. Our problem is much more difficult since one cannot see through the star, and thus only a fraction of the stellar surface is recorded in any single observation. However, preliminary experiments indicate that a major simplification of our present iterative approach should be possible.

We wish to acknowledge the generous assistance in software development provided by Dr. R. Stover, Ms. De Clarke, and Mr. Robert Kibrick. We also wish to thank Mr. Tod Lauer for many useful discussions and software assistance. We are grateful to Dr. R. P. Kraft, Director of Lick Observatory, for sufficient amounts of telescope time. This research was made possible by NSF grants AST 79-16813 and AST 82-10202 to (S.S.V.), and by NSF grant AST 80-17054 to Lick Observatory for the VAX computer system. We are grateful to the foundation for this support.

REFERENCES

- Bartolini, C., Blanco, C., Catalano, S., Cerruti-Sola, M., Eaton, J. A., Guarnieri, A., Hall, D. S., Henry, G. W., Hopkins, J. L., Landis, H. J., Louth, H., Marilli, E., Piccioni, A., Renner, T. R., Rodono, M., and Scaltriti, F. 1983, *Astr. and Ap.* 117, 149.
- Bell, R. A., Eriksson, K., Gustafsson, B., and Nordlund, Å. 1976, *Astr. and Ap. Suppl.* 23, 37.
- Bumba, V., and Howard, R. 1965, *Ap. J.* 141, 1502.
- Chambliss, C. R., Hall, D. S., Landis, H. J., Louth, H., Olson, E. C., Renner, T. R., and Skillman, D. R. 1978, *A.J.* 83, 1514.
- Dorren, J. D., and Guinan, E. F. 1982, *Ap. J.* 252, 296.
- Fekel, F. 1980, *Bull. A.A.S.* 12, 500.
- Fekel, F. 1983, *Ap. J.* 268, 274.
- Feldman, P. A., MacLeod, J. M., and Andrew, B. H. 1979, *I.A.U. Circ.* No. 3385.
- Feldman, P. A., Taylor, A. R., Gregory, P. C., Seaquist, E. R., Balonek, T. J., and Cohen, N. L. 1978, *A.J.* 83, 1471.
- Guinan, E. F., McCook, G. P., Fragola, J. L., and Weisenberger, A. G. 1979, *Inf. Bull. Var. Stars* No. 1723.
- Hall, D. S. 1976, in *I.A.U. Colloquium No. 29*, W. S. Fitch, ed. (Dordrecht: Reidel), p. 287.
- Hartmann, L., Bopp, B. W., Dussault, M., Noah, P. V., and Klimke, A. 1981, *Ap. J.* 249, 662.
- Howard, R. H., and Labonte, B. J. 1981, *Solar Phys.* 74, 131.
- Howard, R. H., and Švestka, Z. 1977, *Solar Phys.* 54, 65.
- Harvey, K. L., Sheeley, N. R., Jr., and Harvey, J. W. 1982, *Solar Phys.* 79, 149.
- Kurucz, R. L. 1979, *Ap. J. Suppl.* 40, 1.
- Levine, R. H. 1977, in *Coronal Holes and High Speed Wind Streams*, J. Zirker, ed. (Boulder: Colorado Associated University Press), p. 103.
- Levine, R. H. 1982, *Solar Phys.* 79, 203.
- Oskanyan, V. S., Evans, D. S., Lacy, C., and McMillan, R. S. 1977, *Ap. J.* 214, 430.
- Penrod, G. D., and Vogt, S. S. 1983, *Pub. A.S.P.* 95, 599.
- Rydgren, A. E., and Vrba, F. J. 1983, *Ap. J.* 267, 191.
- Sarma, M. B. K., and Ausekar, B. D. 1980, *Acta Astr.* 30, 101.
- Soderblom, D. R. 1982, *Ap. J.* 263, 239.
- Timothy, A. F., Krieger, A. S., and Vaiana, G. S. 1975, *Solar Phys.* 42, 135.
- Van Leeuwen, F., and Alphenaar, P. 1982, in *I.A.U. Colloquium No. 71*, M. Rodono and P. Byrne, ed. (Dordrecht: Reidel) (in press).
- Vogt, S. S. 1981a, *Proc. Soc. Photo-Opt. Instrum. Eng.* 290, 70.
- Vogt, S. S. 1981b, *Ap. J.* 250, 327.
- Vogt, S. S. 1982, in *I.A.U. Colloquium No. 71*, M. Rodono and P. Byrne, ed. (Dordrecht: Reidel) (in press).
- Vogt, S. S., and Penrod, G. D. 1982, in *I.A.U. Colloquium No. 71*, M. Rodono and P. Byrne, ed. (Dordrecht: Reidel) (in press).
- Waldmeier, M. 1981, *Solar Phys.* 70, 251.
- Walter, F. M., Gibson, D. M., and Basri, G. S. 1983, *Ap. J.* 267, 665.
- Zirker, J. B. (ed.) 1977, *Coronal Holes and High Speed Wind Streams* (Boulder: Colorado Associated University Press).